

PART-SCALE THERMO-MECHANICAL MODELLING FOR THE TRANSFUSION MODULE IN THE SELECTIVE THERMOPLASTIC ELECTROPHOTOGRAPHIC PROCESS

HAO-PING YEH¹, KENNETH Æ. MEINERT², MOHAMAD BAYAT³ AND JESPER H. HATTEL⁴

¹Department of Mechanical Engineering, Technical University of Denmark, building 425, room 229, Lyngby, Denmark
haoye@mek.dtu.dk

²kemei@mek.dtu.dk

³mbayat@mek.dtu.dk

⁴jhat@mek.dtu.dk

Key words: Part-scale, Thermo-mechanical model, Additive manufacturing, FEM, Flash heating, Selective thermoplastic electrophotographic process

Abstract. *This study proposes a thermo-mechanical model for the transfusion module in the additive manufacturing process, selective thermoplastic electrophotographic process (STEP). The reduced-order method and parametric study are presented, as well.*

1 INTRODUCTION

Additive manufacturing (AM) is a breakthrough approach to industries, potentially relieving the limitation when producing complex geometries with traditional manufacturing processes. Selective thermoplastic electrophotographic process or simply called STEP, is a brand-new AM process proposed by Evolve additive solutions Inc. The STEP process works based on layer-wise manufacturing by fusing super-thin nearly 2D layers produced by electrophotography onto a 3D bulk structure. The principle of the 2D to 3D deposition process in STEP is through heating up both the incoming 2D layer and the bulk material and then applying pressure to fuse the 2D layer onto the already-built component. This deposition module in STEP is known as transfusion. With the two core modules, electrophotographic, and transfusion, STEP could create a fully dense and multi-material part [1,2], and the developers hope that it could be an alternative to injection molding.

In the present work we develop the first numerical model for the STEP process. It is a part-scale thermo-mechanical FE model based on the flash heating (FH) [3,4] method in the commercial software package ABAQUS. FH is a part-scale method, originally developed to solve thermal problems in laser-based AM processes, without truly resolving the interaction between the heat source and the bulk material, but instead uniformly distributing the input energy on the recently-activated meta-layer. Both the part material, as well as the support

material in the STEP machine are considered. The thermal predictions [5,6,7,8] are compared with relevant experimental measurements for validation purposes. A comprehensive manufacturing parametric study is also presented. This modelling approach will potentially pave the way for making a robust digital twin of the STEP process, that later could be integrated in the STEP process itself, serving as a feedback source for real-time correction of the input process parameters for achieving a close to defect-free end-product.

2 NUMERICAL METHODOLOGY

This section focuses on the theories and numerical methods for modelling the transfusion module in the STEP machine. The heat transfer equations including conduction, convection, and radiation are introduced. Furthermore, the concept of the reduced-order method, namely FH, is introduced as well.

2.1 Simulation Scenario

The simulation consists of three subprocesses which are the printing process, cooling down to room temperature, and detaching build. Regarding the transfusion module, the main fusion is to deposit a 2D layer on the moving platform or existing build and fuse them together. Starting from the idle step, the platform moves forwards, and the bulk is heated up because of the bulk heater. Afterward, a new heated layer is added to the substrate by roller press. Lastly, the bulk cools down and moves back to the idle area. The steps and time durations of transfusion are shown in Figure 1.

After the printing process, the whole system is left to stand and cool down to room temperature. Detaching the finished printing build and deactivating the platform is the last subprocess of the work. The latter two subprocesses are schematically shown in Figure 2

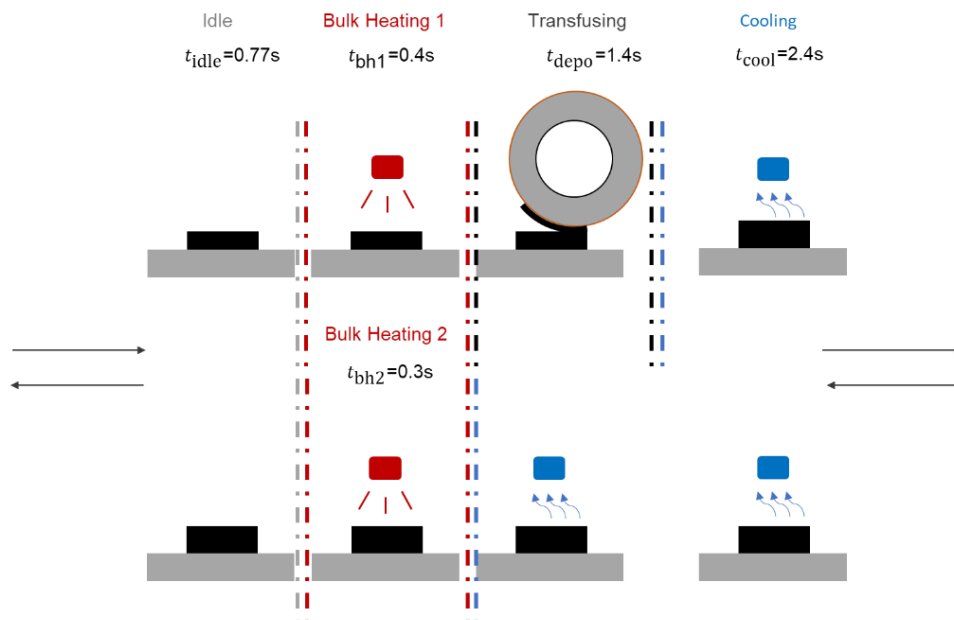


Figure 1: Simulation scenario of printing process

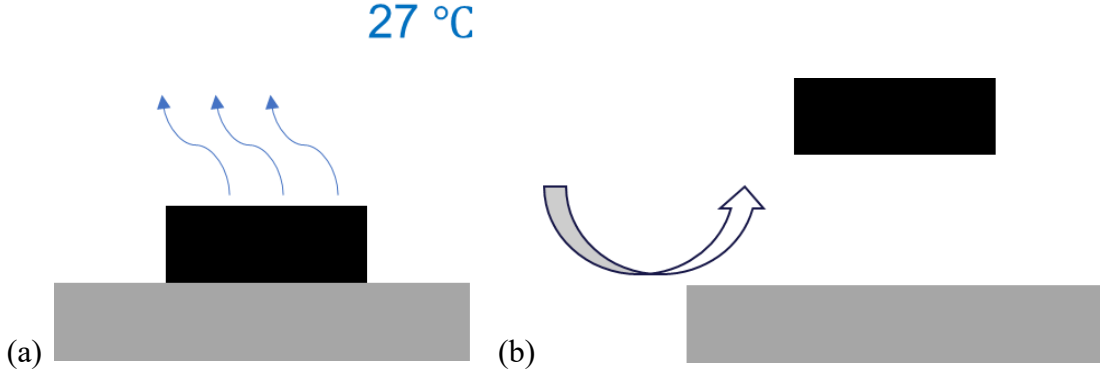


Figure 2: (a) Cooling down to room temperature (b) Detaching the build

2.2 Heat Transfer and Mechanics

For the energy balance, the spatial and temporal distribution of the temperature field is determined by solving the transient heat conduction shown in equation 1,

$$\rho c_p \frac{\partial T}{\partial t} = \frac{\partial}{\partial x} \left(k \frac{\partial T}{\partial x} \right) + \frac{\partial}{\partial y} \left(k \frac{\partial T}{\partial y} \right) + \frac{\partial}{\partial z} \left(k \frac{\partial T}{\partial z} \right) - \rho \Delta H_{met} \frac{\partial r_{liq}}{\partial T} + \dot{Q}''' \quad (1)$$

where $\rho \Delta H_{met} \frac{\partial r_{liq}}{\partial T}$ is the term for energy during melting and solidification. Besides, conducted-heat convection and radiation are also applied in the model based on equation 2.

$$-k \frac{\partial T}{\partial z} = h_{amb} [T - T_{amb}] + \varepsilon \eta [T^4 - T_{amb}^4] \quad (2)$$

In equation 2, h_{amb} , ε , and η are convection coefficient, heat emissivity and Stefan-Boltzmann constant, respectively. In the mechanical model, Hooke's general law shown in equation 3 is used to get stress, strain, and deformation.

$$\sigma_{ij} = \frac{E}{1+\nu} \left[\frac{1}{2} (\delta_{ik} \delta_{jl} + \delta_{il} \delta_{jk}) + \frac{\nu}{1-2\nu} \delta_{ij} \delta_{kl} \right] e_{kl}^{el} \quad (3)$$

2.3 Flash Heating

FH is a reduced-order method to solve thermal load problems, without truly resolving the interaction between the heat source and material. By distributing the heat energy on the top activated meta-layer uniformly, FH reduces the number of mesh and simulation time used and gets acceptable accuracy. The energy equation in FH can be formulated as equation 4.

$$\dot{Q}''' = \frac{U_{\Delta}}{t_{contact}} \quad (4)$$

where U_{Δ} is the volumetric energy for a meta-layer, and $t_{contact}$ is the duration of uniform thermal loading on a meta-layer. The historic temperature profile with respect to three contacting time is shown in Figure 3. The short contacting time comes with higher peak temperature and then drops drastically. The reason the contacting time is too short to transfer heat out and heat accumulates.

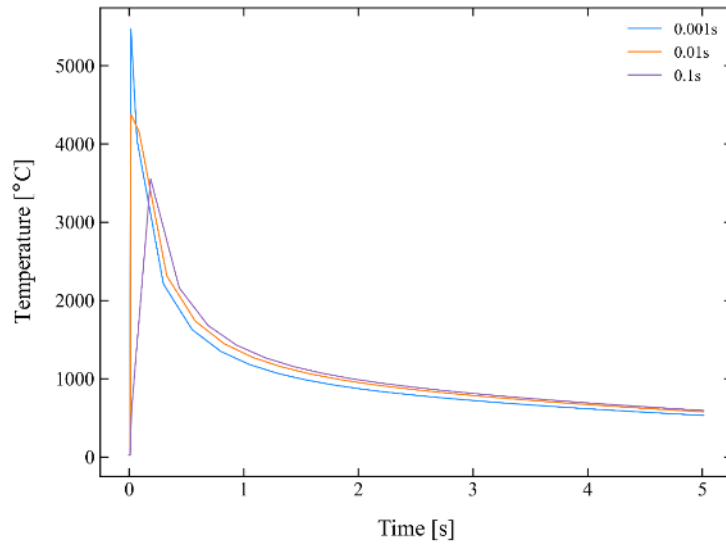


Figure 3: Temperature profile with different exposure time

3 NUMERICAL MODEL SETUP

3.1 Geometry and Material

The geometry used in the study comprises of three parts, i.e., build, substrate, and platform. The dimensions and illustrations are shown in Figure 4.

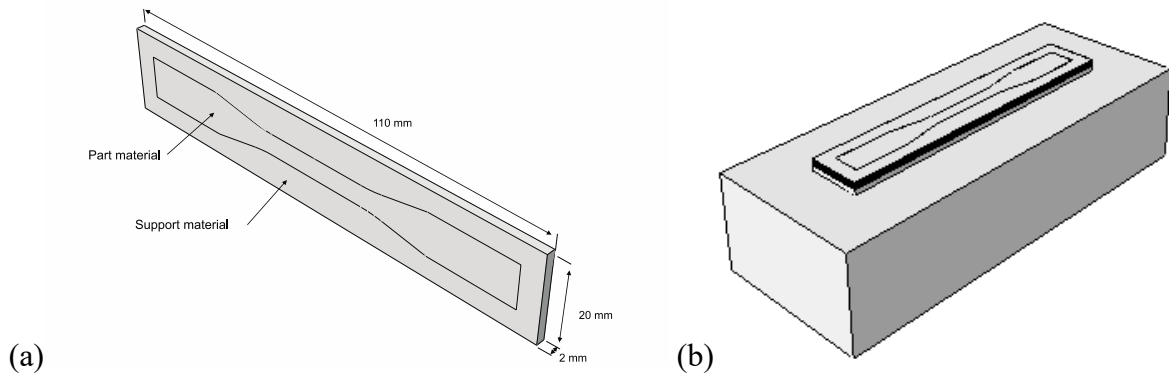


Figure 4: Geometry and dimensions in the simulation (a) Build: single tensile bar and support structure (b) Build, substrate and platform

The multi-material build in this work is made up of part and support material. Both part and support materials are polymer. Substrate and platform are made of support material and steel respectively. Moreover, temperature-dependent thermal properties, e.g., conductivity and

specific heat are measured using a C-Therm thermal penetrator at DTU Geo Laboratory and applied in the model.

3.2 Mesh Size

In order to well resolve the problem and reduce simulation time, different mesh size is specified in different areas shown in Table 1. The build in z-direction uses the finest mesh equal to the thickness of an actual layer because the heat transfer is more significant in deposition direction than others shown in Figure 5.

Table 1: Mesh size in different regions

Region	Mesh size
Platform	10 mm
Substrate	3 mm
Build (xy-direction)	2 mm
Build (z-direction)	16 μm

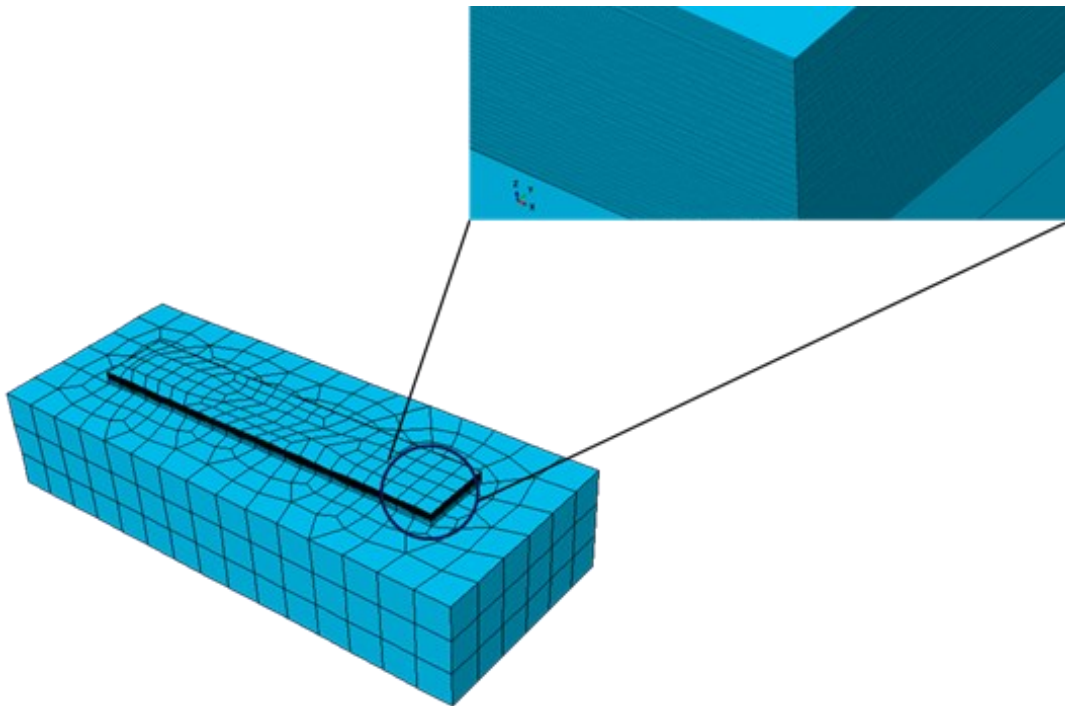


Figure 5: Meshing procedure of the simulation domain

4 SIMULATION RESULT AND DISCUSSION

There are four thermal cameras integrated in the transfusion module to capture the temperature of the top surface of the build. After some postprocessing, we can get the average temperature at idle as a function of time. Figure 6 shows the calibration with our simulation reference. The curve quite fits the thermal data whether in trend or value. The high-fidelity only has a 1.34% mean absolute percentage error. Regarding parametric study, we specify the heat intensity from 2.2×10^4 to 3.1×10^4 W/m² shown in Figure 7. When higher heater intensity is applied, the temperature curve gradually increases because of heat accumulation. On the contrast, lower heat intensity comes with a declining trend, as expected

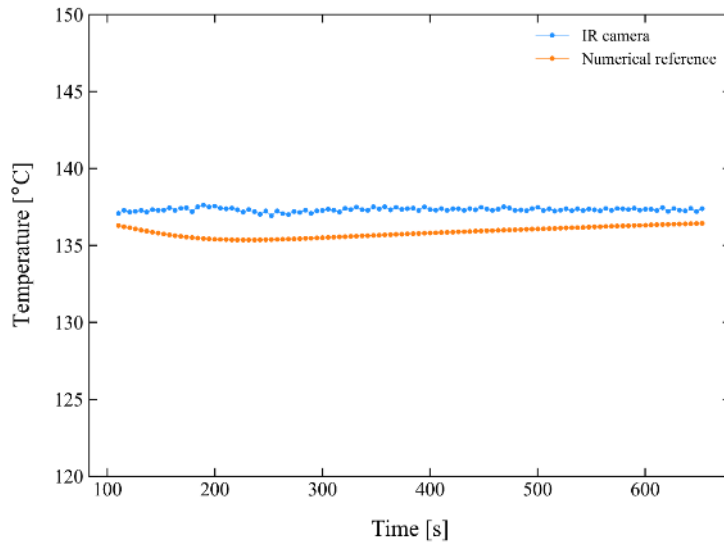


Figure 6: High-fidelity result for part material at every idle step and starts from 100 s.

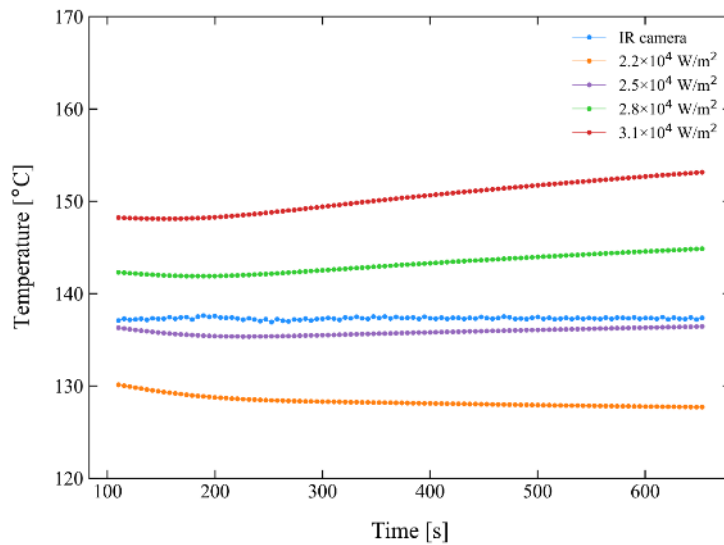


Figure 7: Temperature to time by different powers of heat flux.

Based on the sensor data, one can assume that there is no big deviation in the temperature profile between each layer. Therefore, it is reasonable to extract the simulation results of layers 50th and 51st as an example for illustration. Figure 8 presents the temperature variation during the printing process. Eventually, the build is taken off from the platform and the deformation or warping takes place. Thermal residual stress shown in Figure 9 is induced by thermal cycle and results in these effects. Although the magnitude of the deformation has not yet been validated, the warping defects indeed occur in the actual finished product due to residual stresses.

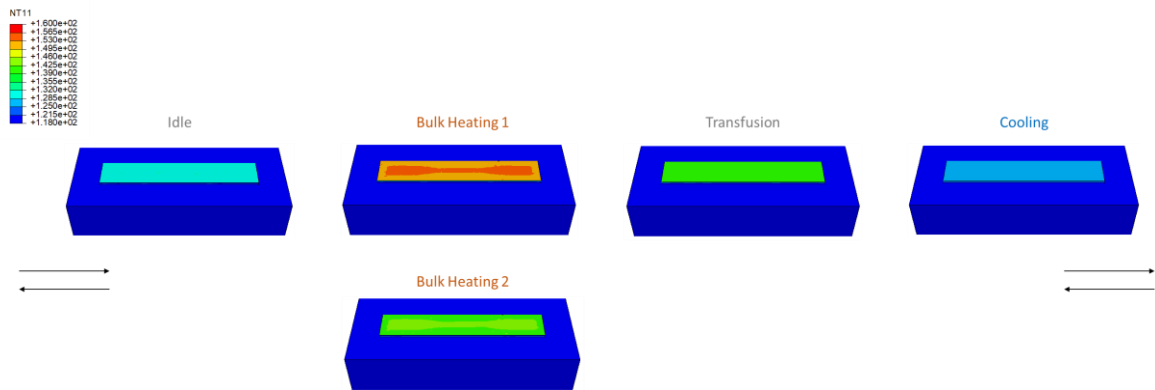


Figure 8: 3D contour of temperature during the 51st layer manufacturing

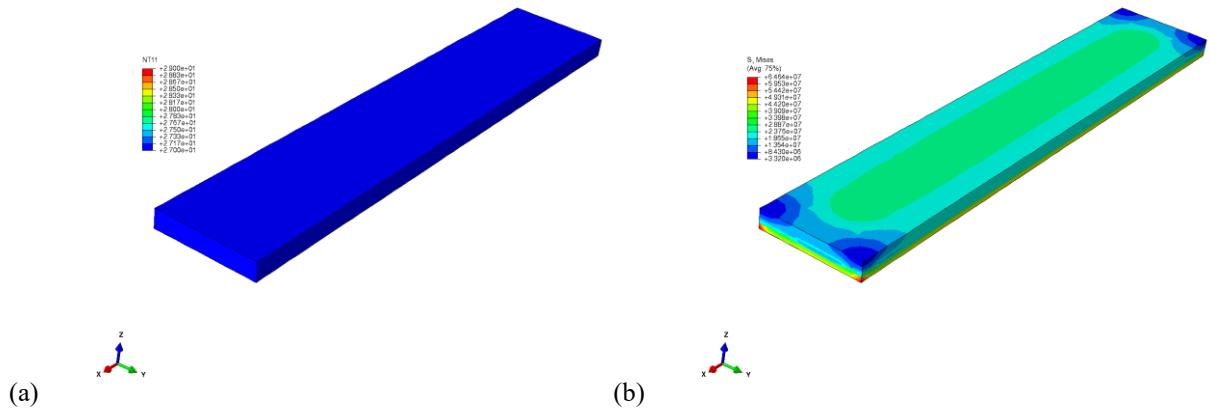


Figure 9: (a) Temperature contour (b) Residual stress of build after cooling down to room temperature

REFERENCES

- [1] T. Stichel, B. Geißler, J. Jander, T. Laumer, T. Frick, and S. Roth, “Electrophotographic multi-material powder deposition for additive manufacturing,” *Journal of Laser Applications*, vol. 30, no. 3, p. 032306, Aug. 2018, doi: 10.2351/1.5040619.
- [2] M. Rafiee, R. D. Farahani, and D. Therriault, “Multi-Material 3D and 4D Printing: A Survey,” *Advanced Science*, vol. 7, no. 12. John Wiley and Sons Inc., Jun. 01, 2020. doi: 10.1002/advs.201902307.
- [3] M. Bayat *et al.*, “Part-scale thermo-mechanical modelling of distortions in Laser Powder Bed Fusion – Analysis of the sequential flash heating method with experimental validation,” *Additive Manufacturing*, vol. 36, Dec. 2020, doi: 10.1016/j.addma.2020.101508.
- [4] K. Ettaieb, S. Lavernhe, and C. Tournier, “A flash-based thermal simulation of scanning paths in LPBF additive manufacturing,” *Rapid Prototyping Journal*, vol. 27, no. 4, pp. 720–734, 2021, doi: 10.1108/RPJ-04-2020-0086.
- [5] D. Ravoori, C. Lowery, H. Prajapati, and A. Jain, “Experimental and theoretical investigation of heat transfer in platform bed during polymer extrusion based additive manufacturing,” *Polymer Testing*, vol. 73, pp. 439–446, Feb. 2019, doi: 10.1016/j.polymertesting.2018.11.025.
- [6] A. Danezis, D. Williams, M. Edwards, and A. A. Skordos, “Heat transfer modelling of flashlamp heating for automated tape placement of thermoplastic composites,” *Composites Part A: Applied Science and Manufacturing*, vol. 145, Jun. 2021, doi: 10.1016/j.compositesa.2021.106381.
- [7] H. Prajapati, D. Ravoori, and A. Jain, “Measurement and modeling of filament temperature distribution in the standoff gap between nozzle and bed in polymer-based additive manufacturing,” *Additive Manufacturing*, vol. 24, pp. 224–231, Dec. 2018, doi: 10.1016/j.addma.2018.09.030.
- [8] A. el Moumen, M. Tarfaoui, and K. Lafdi, “Modelling of the temperature and residual stress fields during 3D printing of polymer composites,” *International Journal of Advanced Manufacturing Technology*, vol. 104, no. 5–8, pp. 1661–1676, Oct. 2019, doi: 10.1007/s00170-019-03965-y.